A Letters Journal Exploring the Frontiers of Physics

May 2019

EPL, **126** (2019) 40004 www.epljournal.org
doi: 10.1209/0295-5075/126/40004

# Pulling cargo increases the precision of molecular motor progress

Aidan I. Brown[1,2] and David A. Sivak[1]

[1] *Department of Physics, Simon Fraser University - Burnaby, BC, V5A1S6 Canada*
[2] *Department of Physics, University of California, San Diego - San Diego, CA 92093, USA*

received 19 March 2019; accepted in final form 21 May 2019
published online 27 June 2019

PACS 05.70.Ln – Nonequilibrium and irreversible thermodynamics
PACS 05.40.-a – Fluctuation phenomena, random processes, noise, and Brownian motion
PACS 87.16.Wd – Intracellular trafficking

**Abstract** – Biomolecular motors use free energy to drive a variety of cellular tasks, including the transport of cargo, such as vesicles and organelles. We find that the widely used "constant-force" approximation for the effect of cargo on motor dynamics leads to a much larger variance of motor step number compared to explicitly modeling diffusive cargo, suggesting the constant-force approximation may be misapplied in some cases. We also find that, with cargo, motor progress is significantly more precise than suggested by a recent result. For cargo with a low relative diffusivity, the dynamics of continuous cargo motion —rather than discrete motor steps— dominate, leading to a new, more permissive bound on the precision of motor progress which is independent of the number of stages per motor cycle.



**Introduction.** – Biomolecular machines, driven by free-energy consumption, perform a variety of cellular roles [1]. Motors, such as kinesin, myosin, and dynein tow cargoes along subcellular filaments for rapid and directed transport [2]. The stochastic dynamics of these motors have been studied for decades [3], with recent experimental work observing their operation with improving resolution [4].

An important aspect of motor dynamics is the response to external forces, as the primary role of many *in vivo* motors is to tow cargoes, which impose drag forces. External forces are frequently modeled as constant across all motor cycles and cycle stages [5–13], recapitulating sophisticated experiments which use feedback to maintain near-constant resisting forces on the forward motion of molecular motors [14–17].

Molecular motors are also excellent systems in which to investigate statistical fluctuations at the nanoscale. Fluctuations in molecular motor progress have been related to the number of stages [6,18–20] and energy dissipation budget [21,22] for each motor cycle.

In this letter we investigate simple theoretical models of molecular motors towing cargo, with cargo represented either implicitly as a constant force or explicitly with diffusive dynamics. We find that constant-force models for cargo do not in general reproduce the step-number distributions of explicit diffusive-cargo models. The step-number Fano factor for diffusive cargo is also substantially less than when predicted solely from motor characteristics [6,18–22]. We demonstrate that diffusing cargo introduces a large number of effective stages to each motor cycle, allowing motors to increase the precision of their progress by pulling cargo, and often rendering the number of motor states irrelevant to the precision of motor progress. Our new, more permissive bound on the precision of motor progress, expressed in eq. (12), only depends on the energy dissipation budget per cycle.

**Model.** – Molecular motor dynamics are commonly described as stochastic transitions between discrete states. For a simple one-state unicyclic model, every forward cycle results in a forward step of the motor and consumption of the free-energy budget $\omega$ per cycle. For "constant-force" motor dynamics (shown schematically in fig. 1(a)), we use static transition rate constants

$$k_{\mathrm{cf}}^{+} = k_{\mathrm{cf}}^{0}\, e^{\omega - \Delta G_{\mathrm{cf}}} \qquad \text{and} \qquad k_{\mathrm{cf}}^{-} = k_{\mathrm{cf}}^{0}, \tag{1}$$

with $k_{\mathrm{cf}}^{+}$ and $k_{\mathrm{cf}}^{-}$ the rate constants of forward and reverse transitions, respectively. $k_{\mathrm{cf}}^{0}$ is a "bare" rate constant, with transition timescale chosen to give $k_{\mathrm{cf}}^{0} = 1$. $\Delta G_{\mathrm{cf}}$ is a constant free-energy difference representing the effect of a load (*e.g.*, towing cargo) on rate constants. $\Delta G_{\mathrm{cf}}$ is frequently set to $f d_{\mathrm{m}}$, with $f$ the constant opposing force and $d_{\mathrm{m}}$ the motor step size. We set

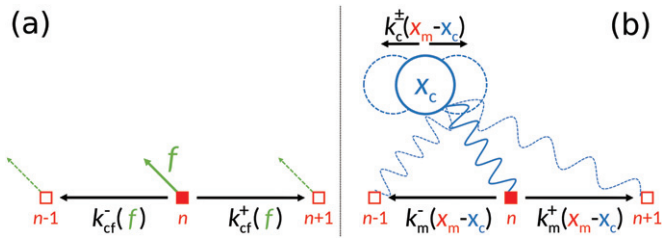


Fig. 1: Constant-force and diffusing-cargo models. (a) Constant-force model. Motor at site $n$ (filled red square) and position $x_\mathrm{m}$ can transition forward to site $n+1$ at rate $k_\mathrm{cf}^{+}$ or reverse to site $n-1$ at rate $k_\mathrm{cf}^{-}$. The rates $k_\mathrm{cf}^{\pm}$ are functions of a constant opposing force $f$. (b) Diffusing-cargo model. The motor and the cargo (blue circle) are linked, so that forward and reverse motor and cargo transition rates $k_\mathrm{m}^{\pm}$ and $k_\mathrm{c}^{\pm}$, respectively, are a function of motor position $x_\mathrm{m}$ and cargo position $x_\mathrm{c}$, which vary with cargo and motor motion.

energies to units of $k_\mathrm{B}T$, for Boltzmann's constant $k_\mathrm{B}$ and temperature $T$.

The transition rate constants in eq. (1) (as well as all other model variations in this work) satisfy microscopic reversibility, quantified by the general detailed balance condition $k_\mathrm{cf}^{+}/k_\mathrm{cf}^{-} = \exp(\Delta G)$ for free-energy difference $\Delta G$, reducing at equilibrium to detailed balance and no net flux. This condition is a standard constraint on rate constants in thermodynamically consistent models of molecular motors [5,9,12,23–26].

The forward transition rate constant in eq. (1) is affected by the load $\Delta G_\mathrm{cf}$, while the reverse rate constant is unaffected. This is a specific limiting case of how load can impact rate constants, as the influence of the load can generally be split between the forward and reverse rate constants [12,23,25]. In the Supplementary Material `Supplementarymaterial.pdf` (SM) ("Reverse-labile motor dynamics"), we show that the opposite extreme, where the load only increases the reverse rate constant and leaves the forward rate constant unchanged, does not change our conclusions.

The motor diffusivity is

$$D_\mathrm{cf} \equiv d_\mathrm{m}^2 \frac{\langle n^2\rangle - \langle n\rangle^2}{2t}, \tag{2}$$

where $n$ is the net number of forward motor steps over time $t$. In terms of rate constants [13],

$$D_\mathrm{cf} = \frac{1}{2}(k_\mathrm{cf}^{+} + k_\mathrm{cf}^{-})d_\mathrm{m}^2. \tag{3}$$

We also consider a similar "diffusing-cargo" kinetic model of a motor taking forward and reverse steps while coupled by a Hookean spring (with spring constant $k_\mathrm{spring}$) to a cargo also taking discrete steps (fig. 1(b)). The motor has transition rate constants

$$k_\mathrm{m}^{+} = k_\mathrm{m}^{0} e^{\omega - \Delta G_\mathrm{sm}^{+}(x_\mathrm{m}-x_\mathrm{c})} \quad \text{and} \quad k_\mathrm{m}^{-} = k_\mathrm{m}^{0}, \tag{4}$$

and the cargo has transition rate constants

$$k_\mathrm{c}^{\pm} = \begin{cases} k_\mathrm{c}^{0}, & \text{if } \Delta G_\mathrm{sc}^{\pm}(x_\mathrm{m}-x_\mathrm{c}) \le 0, \\ k_\mathrm{c}^{0}\, e^{-\Delta G_\mathrm{sc}^{\pm}(x_\mathrm{m}-x_\mathrm{c})}, & \text{if } \Delta G_\mathrm{sc}^{\pm}(x_\mathrm{m}-x_\mathrm{c}) > 0, \end{cases} \tag{5}$$

which provide the standard Hookean response to an applied force in an overdamped medium [27], as derived in the SM ("Overdamped cargo dynamics under force"). $x_\mathrm{m}$ is the motor position and $x_\mathrm{c}$ is the cargo position. $k_\mathrm{m}^{0}$ and $k_\mathrm{c}^{0}$ are the bare rate constants for the motor and cargo, respectively; we choose a timescale such that $k_\mathrm{m}^{0} = 1$. $G_\mathrm{s} = \frac{1}{2}k_\mathrm{spring}(x_\mathrm{m}-x_\mathrm{c})^2$ is the free energy of the spring linking motor to cargo. $\Delta G_\mathrm{sm}^{+} = k_\mathrm{spring}d_\mathrm{m}(x_\mathrm{m}-x_\mathrm{c}) + \frac{1}{2}k_\mathrm{spring}d_\mathrm{m}^2$ is the change in $G_\mathrm{s}$ due to a forward motor step of size $d_\mathrm{m}$, while $\Delta G_\mathrm{sc}^{\pm} = \mp k_\mathrm{spring}d_\mathrm{c}(x_\mathrm{m}-x_\mathrm{c}) + \frac{1}{2}k_\mathrm{spring}d_\mathrm{c}^2$ is the change in $G_\mathrm{s}$ due to a forward (+) or reverse (−) cargo step of size $d_\mathrm{c}$. Cargo diffusivity in the absence of a motor is $D_\mathrm{c} = k_\mathrm{c}^{0}(d_\mathrm{c})^2$, with $d_\mathrm{c}$ held fixed in all simulations and $k_\mathrm{c}^{0}$ varied to adjust $D_\mathrm{c}$. $D_\mathrm{m} = \frac{1}{2}k_\mathrm{m}^{0}d_\mathrm{m}^2(e^{\omega}+1)$ is the diffusivity of a motor without cargo.

The Fano factor for net number $n$ of motor steps taken can be related to the number of stages in a motor cycle $N$ by $\sigma_n^2/\mu_n \ge 1/N$, where $\sigma_n^2$ is the variance of the net forward cycles and $\mu_n$ is the mean number of net forward cycles [6,18–20]. Recent work by Barato and Seifert [21,22] predicts a "thermodynamic uncertainty relation", which further tightens the previous $N$-dependent bound by incorporating the free-energy dissipation budget $\omega$ per cycle:

$$\text{Fano factor} \equiv \frac{\sigma_n^2}{\mu_n} \ge \frac{1}{N}\coth\frac{\omega}{2N}, \tag{6}$$

This bound is for constant-affinity dynamics, and has received substantial attention [28–36]. For a motor cycle with a single step ($N = 1$), eq. (6) becomes an equality, $\sigma_n^2/\mu_n = \coth\frac{\omega}{2}$. Equation (6) applies not only to molecular motors, but to any thermodynamically consistent unicyclic $N$-state Markov model [37].

Our results primarily use relatively small values for the cargo diffusivity, consistent with the low diffusivity of *in vivo* motor cargoes such as vesicles and organelles. A diffusivity of $\sim 10^{-3}\,\mu\mathrm{m}^2/\mathrm{s}$ has been measured for 80 nm-radius beads in the cytosol [38], suggesting vesicles and organelles have diffusivities $D_\mathrm{c} \sim 10^{-5}$–$10^{-3}\,\mu\mathrm{m}^2/\mathrm{s}$. Using experimental kinesin rate constants [39] to estimate $D_\mathrm{m}$ suggests $D_\mathrm{c}/D_\mathrm{m} \sim 10^{-3}$–$10^{-1}$ (see SM).

**Results.** – To explore differences between the constant-force and diffusing-cargo models, we numerically simulate the distribution of the number of net forward steps (hereafter simply the "step number") using the Gillespie algorithm [40], initiated with $x_\mathrm{m} = x_\mathrm{c}$. For a direct comparison, we choose equal bare rates $k_\mathrm{cf}^{0} = k_\mathrm{m}^{0}$ and equal mean motor velocities,

$$v = (k^{+} - k^{-})d_\mathrm{m}. \tag{7}$$

We rearrange the constant-force model rate constants (1) with a mean step number $\mu_n = vt$ to determine the

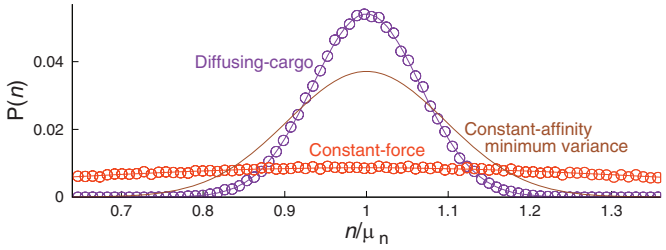


Fig. 2: Anomalously narrow step-number distribution. Step-number probability distribution $P(n)$ as a function of normalized step number $n/\mu_n$. Diffusing-cargo model step-number distribution is narrower than constant-force model and narrower than expected from minimum Fano factor for a constant-affinity cycle. Step-number distribution from $10^5$ samples of numerical diffusing-cargo model (purple circles) after nondimensionalized time $t^* \equiv k_{\rm m}^0 t = 10^3$ with $\omega = 4$, diffusivity ratio $D_{\rm c}/D_{\rm m} = 10^{-3}$, spring constant $k^*_{\rm spring} \equiv k_{\rm spring} d_{\rm m}^2 = 1$, and relative cargo step size $d_{\rm c}/d_{\rm m} = 0.001$, along with Gaussian fit (purple curve). Orange circles: step-number distribution from $10^5$ samples of numerical constant-force model with $\omega = 4$ and equal mean step number $\mu_n$ through choice of $\Delta G_{\rm cf} = 3.8945$. Orange curve: Gaussian distribution predicted by mean $\mu_n$ and eq. (3). Brown curve: Gaussian distribution with mean $\mu_n$ and the constant-affinity minimum variance (6) from [21,22].

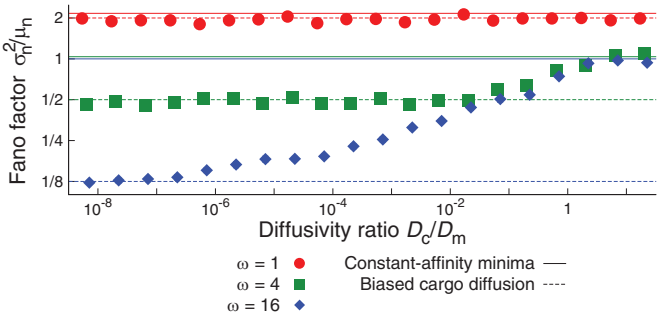


Fig. 3: Motor step-number Fano factor, as a function of cargo-motor diffusivity ratio. Points show numerical diffusing-cargo model averaged over $10^3$ samples after a nondimensionalized time in the range $t^* \equiv k_{\rm m}^0 t = 10^{-4}$–$10^9$ chosen to maintain $\mu_n \sim 100$, thereby providing good statistics and retaining numerical efficiency. Colors indicate different free-energy budgets $\omega$ per cycle. Other parameters are as in fig. 2. Solid lines show motor-controlled behavior of the predicted minimum Fano factor (6) using $N = 1$ and $\omega$ as indicated. Dashed curves show cargo-controlled behavior from discrete cargo steps taken to the continuum limit (12) with motor step size $d_{\rm m}$ held fixed. $D_{\rm c}/D_{\rm m}$ is the ratio of cargo diffusivity $D_{\rm c}$ (in the absence of the motor) to cargo-less motor diffusivity $D_{\rm m}$.

corresponding constant free-energy difference

$$\Delta G_{\rm cf} = \omega - \ln\left(\frac{\mu_n}{d_{\rm m} k_{\rm cf}^0 t} + 1\right). \tag{8}$$

Figure 2 shows the step-number distribution for diffusing-cargo and for constant-force models, with the constant-force model using $\Delta G_{\rm cf}$ from eq. (8) and $\mu_n$ from the diffusing-cargo model. The constant-force step-number variance is predicted by motor dynamics using $\sigma_{\rm cf}^2 = 2 D_{\rm cf} t$. Figure 2 also shows the Gaussian distribution predicted by eq. (6) with the parameters $\omega = 4$ and $N = 1$ used by the numerical models, which does not agree with the constant-force step-number distribution.

Replacing $\omega$ in eq. (6) with a reduced budget $\omega - \Delta G_{\rm cf}$ does reproduce the constant-force variance $\sigma_{\rm cf}^2$, demonstrating that the constant-force model agrees with the minimum Fano factor (6). However, the step-number variance of the diffusing-cargo model in fig. 2 is substantially smaller than both the variance of the constant-force model and the minimum variance from naive application of the uncertainty relation (6). The step-number distributions of fig. 2 suggest that the effect of cargo attached to the motor is not well represented by a constant force and that the cargo allows the motor to circumvent the minimum Fano factor for a constant-affinity cycle (6).

To investigate the discrepancy between the diffusing-cargo model step-number distribution and eq. (6), we find the Fano factor for the diffusing-cargo model across several free-energy budgets $\omega$ and a wide range of cargo diffusivities (fig. 3). At low cargo diffusivity, the diffusing-cargo Fano factor is below the constant-affinity minimum Fano factor (6). For the $N = 1$ cycle used for the diffusing-cargo model, eq. (6) predicts that as $\omega \to \infty$ the Fano factor approaches unity from above —this prediction is unambiguously not followed by the diffusing-cargo model in fig. 3. Instead, the diffusing-cargo Fano factor at low cargo diffusivity moves further below the eq. (6) prediction as the free-energy budget $\omega$ increases, with the Fano factor for free-energy budget $\omega = 16$ approximately 1/8 of that predicted in eq. (6).

We investigate low-diffusivity cargo because of the relatively small diffusivities (compared to nanometer-scale motors) of micron-scale vesicles and organelles, which *in vivo* molecular motors tow up to millimeter distances [41]. For cargo with diffusivity much lower than that of the motor, the distribution of motor positions is near the steady state attained for an unmoving cargo, where $\langle f_{\rm net} \rangle = 0$. Chemical driving imposes a forward force $\langle f_{\rm chem} \rangle = \omega / d_{\rm m}$ on the motor. To maintain the steady state, the motor is opposed by the force from the elastic motor-cargo linker; averaged over the steady-state distribution of motor positions (conditioned on the fixed cargo position), the linker force is $\langle f_{\rm cargo} \rangle = -\omega / d_{\rm m}$. Thus, low-diffusivity cargo experiences an average forward-directed force $\langle f \rangle = \omega / d_{\rm m}$.

Figures 2 and 3 show diffusing-cargo model Fano factors below the mimimum Fano factors for constant-affinity dynamics (6). Here we determine the Fano factor for a cargo under a constant forward force, treating a discrete step of the cargo itself as a single-stage cycle. If the cargo takes steps of size $d_{\rm c}$, with bare rate $k_{\rm c}^0$, its forward and reverse rate constants under constant force $f$ are

$$k_{\rm c}^+ = k_{\rm c}^0 \qquad \text{and} \qquad k_{\rm c}^- = k_{\rm c}^0 e^{-f d_{\rm c}}. \tag{9}$$

Cargo under constant force has velocity and diffusivity expressions analogous to eqs. (7) and (3), respectively; combining these with flat-landscape cargo diffusivity $D_c = k_c^0 d_c^2$ gives the mean and variance for cargo position under constant force,

$$\mu_c = d_m \mu_n = \frac{D_c t}{d_c}(1 - e^{-f d_c}), \tag{10a}$$

$$\sigma_c^2 = d_m^2 \sigma_n^2 = D_c t(1 + e^{-f d_c}). \tag{10b}$$

The Fano factor is then (with $f = \omega/d_m$)

$$\frac{\sigma_n^2}{\mu_n} = \frac{d_c}{d_m} \coth \frac{\omega d_c}{2 d_m}. \tag{11}$$

Substituting $d_c = d_m/N$ recovers (6). For continuous cargo motion, $d_c \to 0$, simplifying (11) to

$$\frac{\sigma_n^2}{\mu_n} = \frac{2}{\omega}. \tag{12}$$

In fig. 3, eq. (12) closely matches the numerical Fano factors for the diffusing-cargo model at low cargo diffusivity, demonstrating that treating cargo motion as a driven cycle leads to accurate prediction of the motor variance. For low cargo diffusivity, slow cargo movement increases the number $N$ of effective stages per motor cycle. Using the minimum Fano factor of Barato and Seifert (6), the increase in $N$ reduces the variance, but the variance cannot fall below the minimum required by budget $\omega$.

In fig. 3, increasing cargo diffusivity causes the motor step-number Fano factor to transition from the cargo-controlled description of eq. (12), to the motor-controlled prediction of eq. (6) as the cargo diffusivity reaches the cargo-less motor diffusivity $D_m$. Larger budgets $\omega$ cause wider transitions between cargo-controlled and motor-controlled Fano factors, because higher motor velocity breaks the stationary-cargo approximation at lower $D_c/D_m$.

Figure 4 shows that for $D_c/D_m \ll 1$, the motor velocity and diffusivity are predicted by treating the motor-cargo system as cargo pulled by a constant force, while for $D_c/D_m \gg 1$, $\mu_n$ and $\sigma_n^2$ are predicted by treating the system as a cargo-less motor. Although fig. 3 shows that low cargo diffusivity leads to a decreased Fano factor (possibly construed as improved performance), fig. 4 is a reminder that this cargo-induced precision gain comes at the cost of lower velocity.

We chose a Hookean spring to link motor and cargo. However, our results are robust to variation of several linker properties, such as increased dimensionality of cargo motion, nonzero rest length, finite extensibility, and stiffer spring constant (see SM). A previous Langevin model for molecular motors pulling cargo, with force directly determining velocity, finds different behavior in different viscosity regimes [42] (analogous to varying cargo diffusivity), further reinforcing that our findings do not depend on model details.

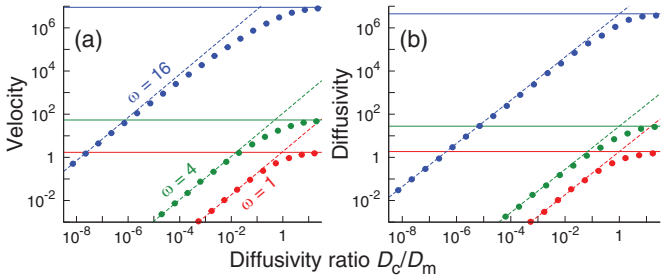


Fig. 4: Motor velocity and diffusivity are controlled by cargo dynamics when cargo diffusivity is low. (a) Motor velocity $\mu_n d_m/t^*$. (b) Motor diffusivity $\sigma_n^2 d_m^2/(2t^*)$. Points are from the numerical diffusing-cargo model averaged over $10^3$ samples, with variable cargo diffusivity and $\omega$ as indicated. Other parameters are as in fig. 3. Solid lines show motor-controlled behavior of a motor without cargo, with $k_m^+ = e^\omega$ and $k_m^- = 1$. Dashed lines show cargo-controlled behavior of biased cargo diffusion (10).

We have used motor rate constants (4) for which chemical and spring free energies affect the forward, but not the reverse, transitions [25,26]. When instead free energies only affect the motor's reverse transition rates, similar Fano factors are produced (see SM).

**Discussion.** – We have investigated the step-number distribution for simple models of molecular motors carrying out their primary role of towing cargo. We examine both a constant-force model representing cargo in a mean-field manner as reducing the driving force biasing forward motion, and a diffusive-cargo model linking the motor to cargo with its own explicit dynamics.

Although constant-force models of molecular motor operation are widely used [5–13], they do not accurately reproduce the step-number distribution of diffusive-cargo models, with a model explicitly including diffusive cargo having a substantially lower variance (fig. 2). The step-number distribution for the constant-force model is consistent with the minimum Fano factor (6) derived by Barato and Seifert [21,22], because the constant-force model satisfies the constant-affinity assumption underpinning eq. (6). This constant-affinity condition is also fulfilled by the diffusing-cargo model when the cargo dynamics are faster than the motor dynamics, allowing the cargo to quickly relax to near equilibrium following a motor step. However, the diffusive-cargo model produces —for sufficiently large free-energy budget $\omega$ and low cargo diffusivity $D_c$— a significantly lower Fano factor than expected from a naive application of (6) (fig. 3). Such a low Fano factor occurs because the attachment of diffusive cargo to the motor changes motor dynamics such that the affinity is not constant (*i.e.*, the ratio of forward to reverse rate constants of the motor depends on the relative locations of motor and cargo), thus violating the constant-affinity assumption in Barato and Seifert [21,21]. The attachment of diffusive cargo to a molecular motor can thus increase the precisionof forward motor progress.

For low cargo diffusivity, the cargo moves very slowly, and forward progress is well approximated by assuming the *motor* provides a constant forward force on the *cargo*. This contrasts with analogous constant-force models that assume the cargo imposes a constant force on the motor. This change in behavior when switching from high to low cargo diffusivity regimes can also be achieved by switching from low to high viscosity while leaving cargo unchanged [42].

Our derived Fano factor for biased cargo diffusion (12) is predictive of diffusive-cargo model behavior when cargo diffusivity is low (fig. 3), and represents a new, more permissive bound on the precision of motor progress. Equation (12) eliminates the number of stages in a motor cycle from consideration as a factor limiting motor precision, and is equal to the Barato-Seifert Fano factor (6) for $N$ equal to the very large effective number of cargo steps to complete a single motor step (11). Thus, low-diffusivity cargo allows the motor to achieve the minimum Fano factor of a cycle with many stages. The minimum Fano factor of Barato and Seifert (6) must be applied carefully, and for a composite system of a motor linked to other elements, the entire system must be considered.

Molecular motor kinetic rates inferred from experiment are consistent with those that improve motor precision in our simulations. For example, Vu *et al.* [39] fit rate constants for a one-stage model of kinesin, suggesting a free-energy budget per cycle of $\sim 6 k_{\mathrm{B}} T$ (substantially lower than the expected $20 k_{\mathrm{B}} T$ from ATP hydrolysis). This budget is sufficiently large to produce a step-number Fano factor for a motor with *in vivo* cargos ($D_{\mathrm{c}}/D_{\mathrm{m}} \approx 10^{-3}$) that significantly differs from that of a motor without cargo (fig. 3).

Potentially comparable experiments on biomolecular motor systems [14,18,43], although pulling cargo ($\sim$50 nm beads) significantly larger than the motor itself, only explore diffusivity ratios of $D_{\mathrm{c}}/D_{\mathrm{m}} \sim 200$, which for our model is too large to observe increased precision of motor progress (fig. 3). These experiments are performed in room temperature water with viscosity $\sim 10^{-3}\,\mathrm{Pa \cdot s}$; cellular interiors are $10^5$–$10^6\times$ more viscous [38,44], sufficiently suppressing the diffusivity of typical cellular cargo such that we would predict increased motor precision. A comparison of step-number Fano factor between a cargo-less motor and an identical motor with low-diffusivity cargo, both in high-viscosity conditions, would distinguish intrinsic motor behavior from the cargo-induced Fano factor decrease our work predicts, but we are unaware of any existing studies with such data.

The constant-force model assumes that the free-energy difference $\Delta G_{\mathrm{cf}}$ modeling the effect of cargo is diverted to moving the motor against the constant force, and is unavailable to bias motor dynamics in the forward direction. For a motor pulling diffusive cargo, free energy is initially stored in the elastic linker connecting motor and cargo, but is ultimately dissipated as the cargo relaxes, and would not generally be available for reversible extraction at a later time [45]. The assumption that the free energy is stored, when it is instead dissipated, leads to an underestimate of the free-energy dissipation budget per motor cycle, which is remedied by explicit consideration of cargo. The elastic restoring force and energy storage of the linker play an important role for a reduced cargo-controlled Fano factor, as we demonstrate with "deterministic" cargo dynamics (an unphysical cargo with drag but not stochastic diffusion) in the SM.

*In vivo* motors often work in teams of two or more to pull cargo through the cell [46]. Following eqs. (10)–(12) with two motors, we expect a halved Fano factor of $\sigma_n^2/\mu_n = 1/\omega$, consistent with previous work exploring multiple motors [42], suggesting multiple motors would further increase the precision of motor progress.

* * *

The authors thank Miranda Louwerse (SFU Chemistry), Steve Large, John Bechhoefer, and especially Nancy Forde (SFU Physics) for useful discussions and feedback. This work was supported by a Natural Sciences and Engineering Research Council of Canada (NSERC) Discovery Grant, by funds provided by the Faculty of Science, Simon Fraser University through the President's Research Start-up Grant, by a Tier II Canada Research Chair, and by WestGrid (`www.westgrid.ca`) and Compute Canada Calcul Canada (`www.computecanada.ca`).

REFERENCES

[1] Alberts B., *Cell*, **92** (1998) 291.
[2] Vale R. D., *Cell*, **112** (2003) 467.
[3] Hackney D. D., *Annu. Rev. Physiol.*, **58** (1996) 731.
[4] Isojima H., Iino R., Niitani Y., Noji H. and Tomishige M., *Nat. Chem. Biol.*, **12** (2016) 290.
[5] Fisher M. E. and Kolomeisky A. B., *Proc. Natl. Acad. Sci. U.S.A.*, **96** (1999) 6597.
[6] Fisher M. E. and Kolomeisky A. B., *Proc. Natl. Acad. Sci. U.S.A.*, **98** (2001) 7748.
[7] Thomas N., Imafaku Y. and Tawada K., *Proc. R. Soc. Lond. B*, **268** (2001) 2113.
[8] Qian H., *Phys. Rev. E*, **69** (2004) 012901.
[9] Lau A. W. C., Lacoste D. and Mallick K., *Phys. Rev. Lett.*, **99** (2007) 158102.
[10] Hinczewski M., Tehver R. and Thirumalai D., *Proc. Natl. Acad. Sci. U.S.A.*, **110** (2013) E4059.
[11] Qian H., Kjelstrup S., Kolomeisky A. B. and Bedeaux D., *J. Phys.: Condens. Matter*, **28** (2016) 153004.
[12] Wagoner J. A. and Dill K. A., *J. Phys. Chem. B*, **120** (2016) 6327.
[13] Hwang W. and Hyeon C., *J. Phys. Chem. Lett.*, **8** (2017) 250.
[14] Visscher K., Schnitzer M. J. and Block S. M., *Nature*, **400** (1999) 184.
[15] Clemen A. E.-M., Vilfan M., Jaud J., Zhang J., Barmann M. and Rief M., *Biophys. J.*, **88** (2005) 4402.

[16] Clancy B. E., Behnke-Parks W. M., Andreasson J. O. L., Rosenfeld S. S. and Block S. M., *Nat. Struct. Mol. Biol.*, **18** (2011) 1020.
[17] Nicholas M. P., Hook P., Brenner S., Wynne C. L., Vallee R. B. and Gennerich A., *Nat. Commun.*, **6** (2015) 6206.
[18] Svoboda K., Mitra P. P. and Block S. M., *Proc. Natl. Acad. Sci. U.S.A.*, **91** (1994) 11782.
[19] Koza Z., *Acta Phys. Pol. B*, **33** (2002) 1025.
[20] Koza Z., *Phys. Rev. E*, **65** (2002) 031905.
[21] Barato A. C. and Seifert U., *Phys. Rev. Lett.*, **114** (2015) 158101.
[22] Barato A. C. and Seifert U., *J. Phys. Chem. B*, **119** (2015) 6555.
[23] Schmiedl T. and Seifert U., *EPL*, **83** (2008) 30005.
[24] Astumian R. D., *Biophys. J.*, **108** (2015) 291.
[25] Brown A. I. and Sivak D. A., *Proc. Natl. Acad. Sci. U.S.A.*, **114** (2017) 11057.
[26] Brown A. I. and Sivak D. A., *J. Phys. Chem. B*, **122** (2018) 1387.
[27] Mazonka O. and Jarzynski C., arXiv:cond-mat/9912121 (1999).
[28] Hyeon C. and Hwang W., *Phys. Rev. E*, **96** (2017) 012156.
[29] Gingrich T. R., Horowitz J. M., Perunov N. and England J. L., *Phys. Rev. Lett.*, **116** (2016) 120601.
[30] Polettini M., Lazarescu A. and Esposito M., *Phys. Rev. E*, **94** (2016) 052104.
[31] Gingrich T. R. and Horowitz J. M., *Phys. Rev. Lett.*, **119** (2017) 170601.
[32] Proesmans K. and Van den Broeck C., *EPL*, **119** (2017) 20001.
[33] Sartori P. and Tu Y., *Phys. Rev. Lett.*, **115** (2015) 118102.
[34] Nguyen M. and Vaikuntanathan S., *Proc. Natl. Acad. Sci. U.S.A.*, **113** (2016) 14231.
[35] Ouldridge T. E., Govern C. C. and Rein ten Wolde P., *Phys. Rev. X*, **7** (2017) 021004.
[36] Hwang W. and Hyeon C., *J. Phys. Chem. Lett.*, **9** (2018) 513.
[37] Pietzonka P., Barato A. C. and Seifert U., *J. Phys. A: Math. Theory*, **49** (2016) 34LT01.
[38] Luby-Phelps K., *Int. Rev. Cytol.*, **192** (2000) 189.
[39] Vu H. T., Chakrabarti S., Hinczewski M. and Thirumalai D., *Phys. Rev. Lett.*, **117** (2016) 078101.
[40] Gillespie D. T., *J. Phys. Chem.*, **81** (1977) 2340.
[41] Hirokawa N., Noda Y., Tanaka Y. and Niwa S., *Nat. Rev. Mol. Cell Biol.*, **10** (2009) 682.
[42] McKinley S. A., Athreya A., Fricks J. and Kramer P. R., *J. Theor. Biol.*, **305** (2012) 54.
[43] Cappello G., Badoual M., Ott A., Prost J. and Busoni L., *Phys. Rev. E*, **68** (2003) 021907.
[44] Caragine C. M., Haley S. C. and Zidovska A., *Phys. Rev. Lett.*, **121** (2018) 148101.
[45] Wang H. and Oster G., *Europhys. Lett.*, **57** (2002) 134.
[46] Mallik R., Rai A. K., Barak P., Rai A. and Kunwar A., *Trends Cell Biol.*, **23** (2013) 575.